Injection Heights of Biomass Burning Debris Estimated From WSR-88D Radar Observations

Thomas A. Jones and Sundar A. Christopher

***Abstract*—Understanding the vertical distribution of aerosols is critical to accurately determining their effects on air quality. Since current tools for obtaining this information have limited spatial and temporal coverage, we explore the use of Doppler radar data for obtaining the injection heights of biomass burning debris (BBD) produced from large fires in southern Georgia during Spring 2007. Due to their submicrometer sizes, the smoke aerosols are not detected by the radar. Therefore, we use BBD as a possible surrogate for aerosol height since smoke aerosols are often collocated with the debris. Using 32 h of Weather Surveillance Radar-1988 Doppler (WSR-88D) radar data from Jacksonville, FL, between May 23 and 25, 2007, the injection heights of BBD ($D \sim 1$ mm) are calculated. Our analysis indicates that the maximum injection height is $\sim$5 km for the strongest fire, with a mean injection height of 3 $\pm$ 1.0 km. Maximum injection heights are present between 1800 and 0000 UTC, during the late afternoon periods when both the intensity of the fire (based on radar information) and the convective mixing are greatest. The injection heights estimated from this approach represent the first step at providing inputs for future air-quality forecasting applications within numerical simulations, particularly ones that require diurnal information.**

***Index Terms*—Aerosols, air pollution, injection height, radar, smoke.**

I. Introduction

ONE OF THE major issues in particulate-matter air-quality monitoring and forecasting is the lack of accurate measurements of the vertical distribution of aerosols that is vital to local and downstream air-quality conditions [1]. What data that are available generally originate from case study experiments or individual lidar locations. Neither of these data sources provide the necessary spatial and temporal resolution to adequately resolve aerosol profiles on a regional basis. Even if they could, much of these data are not available in a near real-time fashion. The launch of the Cloud-Aerosol Lidar and Infrared Pathfinder Satellite Observation (CALIPSO) satellite and its accompanying downward pointing lidar, which is sensitive to both aerosol and cloud layers, provides another source of data for aerosol profiles [2]. However, the small swath width ($\sim$70 km) limits the coverage of any one location, and since the overall temporal and spatial coverage of these data is limited, the analysis of short-term trends in the vertical distributions of aerosols and their affects on downstream air quality has proven to be problematic.

On a regional scale, the changes in air quality are both functions of local aerosol sources and aerosols transported from large distances from the source. One example is aerosols from biomass burning fires that can loft large amounts of particulate matter several kilometers into the atmosphere as a result of localized instability and increased buoyancy, which is produced by the intense heat of the fire [3]. For example, Kahn *et al.* [4] estimated aerosol plumes extending upward of 5 km above the surface using the Multiangle Imaging SpectroRadiometer (MISR) stereo height observations of a wildfire in Oregon. These plumes are often associated with pyro-cumulus, which form as a result of the combination between the heat-induced updrafts that transport warm moist parcels laden with large concentrations of smoke aerosols acting as cloud condensation nuclei that reaches as high as 10 km into the atmosphere under the most extreme circumstances [5], [6].

Since aerosols are being injected into the atmosphere above the boundary layer, they can be transported hundreds of kilometers downstream before descending and lowering the surface air quality. The maximum height to which substantial aerosols are transported at the source is known as the aerosol injection height, which can be sampled from satellite data from instruments such as CALIPSO and MISR among others [7], [8]. If this parameter is known, then the probability of skillful air-quality forecasts downstream of the fire event can be improved [1]. However, there remain few objectives and near real-time observations of injection height, requiring greater creativity in the use of currently available observation tools.

One currently underutilized tool for sampling the injection height is the Doppler radar. For intense burning, the biomass burning debris (BBD) that lofted into the atmosphere is large enough to be detected by precipitation radars such as the Weather Surveillance Radar-1988 Doppler (WSR-88D) network in the U.S. It is important to note that precipitation radars such as the WSR-88D are not sensitive to smoke aerosol-sized particles themselves ($D < 10\ \mu$m), but rather the larger ash and burnt debris ($D \sim 1$ mm) that also lofted into the atmosphere [6], [9], [10]. The WSR-88D data between May 23 and 25, 2007 in southern Georgia are used to address the ability of WSR-88D radars at sampling and quantifying the injection height of BBD [9]. This time period represents a subset of a two-month-long fire event occurring in the southeastern U.S. between mid-April and mid-June 2007. The period between May 23 and 25 was selected due to the excellent radar representation of the fires and the lack of significant precipitation in the region. The latter is important since the radar cannot discriminate between fire signatures and precipitation without human intervention or

Manuscript received June 13, 2008; revised November 28, 2008 and December 31, 2008. First published April 21, 2009; current version published July 23, 2009. This work was supported in part by the National Oceanic and Atmospheric Administration (NOAA) air quality grants and in part by a National Aeronautics and Space Administration (NASA) Cloud-Aerosol Lidar and Infrared Pathfinder Satellite Observation (CALIPSO) science team grant.

The authors are with the Department of Atmospheric Sciences, The University of Alabama in Huntsville, Huntsville, AL 35805-1912 USA (e-mail: tjones@nsstc.uah.edu).

Color versions of one or more of the figures in this paper are available online at http://ieeexplore.ieee.org.

Digital Object Identifier 10.1109/TGRS.2009.2014225

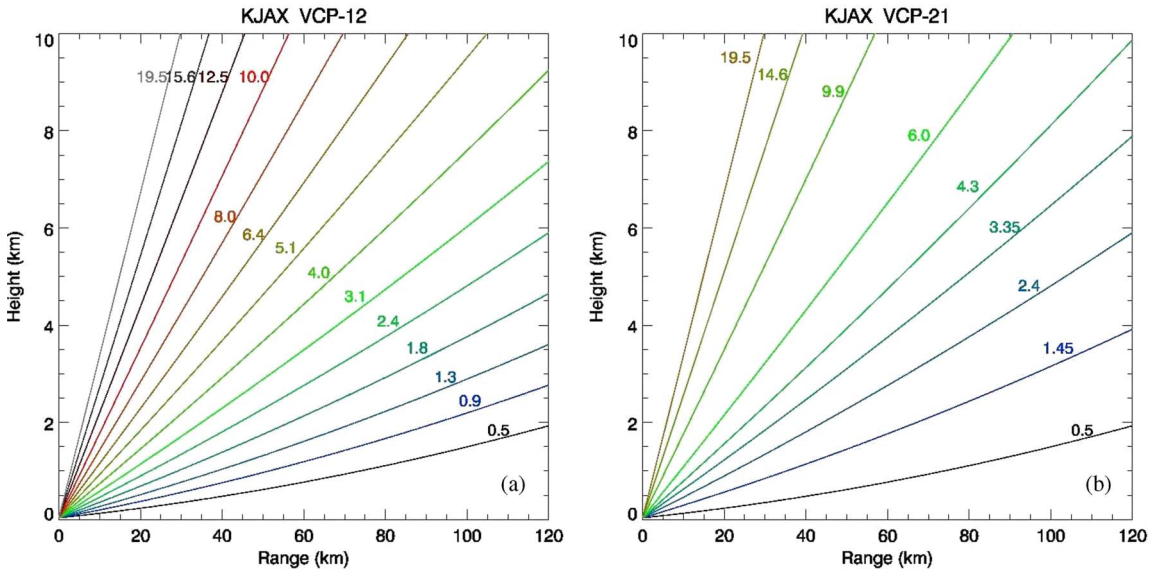

Fig. 1. Centerline heights (ASL) for all elevation scans used by (a) VCP-12 and (b) VCP-21 as a function of range from the Jacksonville, FL (KJAX) WSR-88D radar.

polarimetric radar observations [11]. If precipitation is occurring in the vicinity of a smoke plume, then the radar returns from the water drops will likely dominate anything produced from the fire itself. Radar data are combined with aerosol and cloud observations from the Moderate Resolution Imaging Spectroradiometer (MODIS) and CALIPSO data to qualitatively examine the relationships between the radar-derived BBD characteristics and their relationship to smoke aerosol concentrations. This paper represents the initial effort into using radar-detected BBD as a surrogate for detecting the injection heights of smoke plumes.

II. Data and Methodology

The WSR-88D network consists of approximately 150 operational radars spread out throughout the U.S. and operated by the National Oceanic and Atmospheric Administration National Weather Service. The WSR-88D is an active S-band (10 cm) precipitation radar, with an azimuthal resolution of 1° and a range bin of 1 km, providing a 3-D data volume every 5–6 min [12]. A WSR-88D may be operated in one of the several volume coverage patterns (VCPs) that define the number and height of each scan elevation encompassing a single volume of data [12]. The WSR-88D was designed to detect precipitation-sized hydrometeors ($D > 100\ \mu$m) out to a range of 230 km from backscattered electromagnetic energy in the microwave spectrum. The returned energy is converted into water equivalent reflectivity (dBZ), which is proportional to the sixth power of an object's diameter. As a result, small concentrations of large objects will result in higher reflectivity values compared to large concentrations of small targets. Velocity relative to the radar (radial velocity, in meters per second) is retrieved by sampling the Doppler shift of the returned radar pulse [13]. These radars are also sensitive to large gradients in the refractive index of the atmosphere when they are on the order of one-half the wavelength of the radar pulse or smaller. This phenomenon, which is known as Bragg scattering, results from strong gradients in relative humidity and to a lesser extent temperature resulting from turbulence, which is produced in abundance near a fire. However, Jones *et al.* [10], using polarimetric observations of an apartment fire, noted that particle scattering by BBD was likely the predominant source of reflectivity returns. The radar reflectivity and velocity characteristics of BBD from the Georgia fires are used to estimate their spatial and vertical distributions.

We obtained 32 h (from 2200 UTC on May 23 to 0600 UTC on May 25) of level-2 WSR-88D radar data from Jacksonville, FL, radar (KJAX) to sample the BBD produced by the fires in Georgia. Fire locations are obtained from the geostationary Wildfire Automated Biomass Burning Algorithm (WFABBA) product from GOES-12 [14]. The major fires are located approximately 80–100 km west–northwest of the radar location. During this period, the radar was operated in two modes, both of which are considered precipitation modes: VCP-12, prior to 0900 UTC on May 24; and VCP-21 thereafter. When operated in VCP-12 mode, radar data are collected at 14 elevation angles every 4.5 min, providing greater vertical and temporal resolution compared VCP-21, which collects data for nine elevation scans every 6 min. Fig. 1 shows the height above mean sea level (ASL) of the beam centerline for all elevations of VCP-12 (a) and VCP-21 (b). Recall that the fires are located between 80 and 100 km from the radar at this time, which means that the BBD must exceed at least ∼1.5 km in height to be detected by the lowest elevation scan (0.5°) plotted in Fig. 1.

To objectively determine the injection height from WSR-88D data, we use a modified version of the storm cell identification and tracking (SCIT) algorithm, which was designed to detect and report the spatial and temporal characteristics of individual storm cells [15]. SCIT operates by analyzing 2-D slices of a reflectivity field at a particular time and determining regions of contiguous reflectivity returns exceeding a certain threshold (operationally 30 dBZ). This process is repeated for all levels (or elevation scans when only a single radar is used), producing a database of 2-D reflectivity centroids. SCIT combines these 2-D centroids into 3-D storm cell detections by collocating individual 2-D centroids from different elevations. The SCIT algorithm reports many storm parameters including volume coverage, base and maximum heights, height, and value of

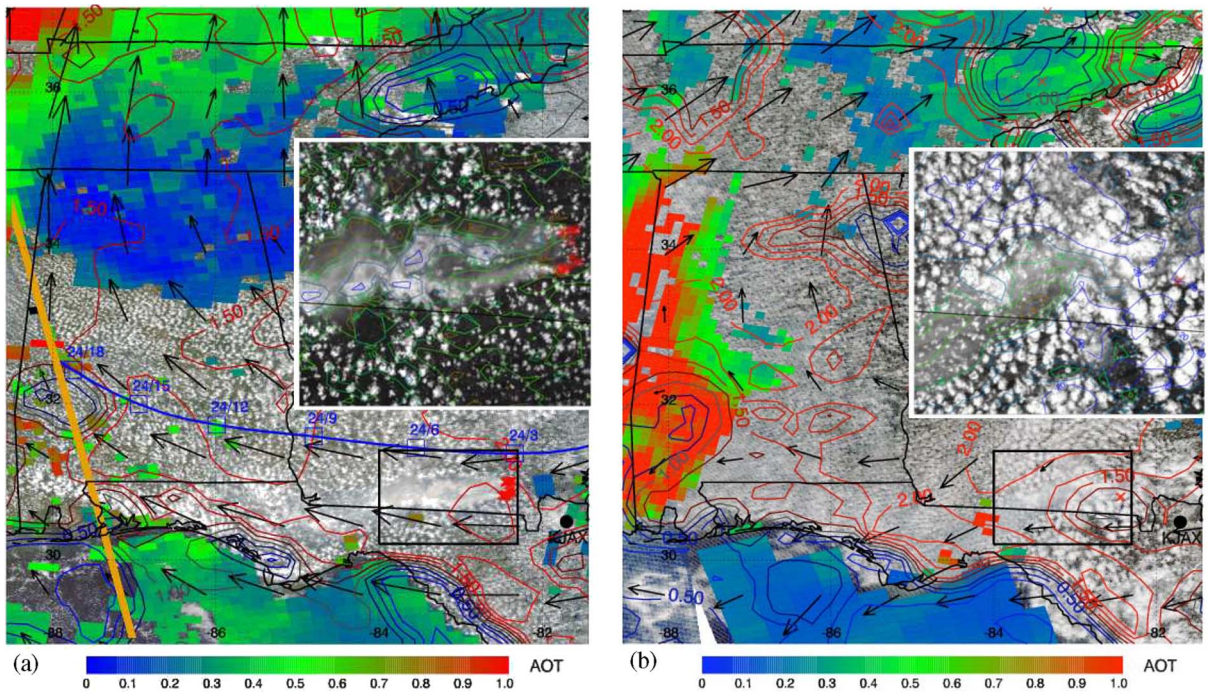

Fig. 2. (a) MODIS 1-km false color image from Aqua at approximately 1900 UTC on May 24, 2007, showing the smoke plume and surrounding cloud field. MODIS level 2 AOTs from Terra and Aqua between 1600 and 1900 UTC are overlaid where valid retrievals occur. Note that clouds prevent aerosol retrievals near where the fires are located and along a portion of the CALIPSO track. Wind vectors at 800 hPa at 1800 UTC on May 24 are shown and indicate a general east-to-west flow. The corresponding RUC-derived boundary layer heights in 0.5-km intervals are contoured on the main image. GOES fire pixels for May 24, 2007 are plotted as red "X"s. The orange line represents the CALIPSO overpass from 1914 UTC on May 24. HYSPLIT back-trajectory analysis starting at 1900 UTC on May 24 (blue) initialized at 32.5° N and 88.0° W for a parcel located at 2 km and run backward in time at 3-h intervals. The inset uses the 250-m MODIS visible channel for better identification of the relative location of the fires and downstream smoke plumes. The width of the inset corresponds to a distance of approximately 160 km. Contours of MYD06 cloud top temperature are overlaid, indicating temperatures at or below -15 °C. (b.) Same as (a) but for 1800 UTC on May 25, but without the CALIPSO track and back-trajectory analysis.

maximum reflectivity, and whether it is collocated with any rotational velocity features [15]. The maximum height parameter, or storm-top, defines the highest level at which reflectivity greater than a predefined threshold is detected, which for this paper is defined as the injection height. Fortunately, BBD often exhibits similar characteristics to those observed in supercell thunderstorms, just on a smaller and less intense scale. To detect these plumes, we modified SCIT to detect "storms" using reflectivity thresholds as low as 10 dBZ compared to the 30-dBZ value used during operations. This increases the algorithm's sensitivity to the weaker reflectivity returns associated with BBD.

During this period, no significant precipitation features were present after 2200 UTC on May 23 near the location of the fires based on the analysis of the radar and surface-based meteorological data available. To ensure that the detections produced by SCIT are indeed from BBD, we compared their location with GOES-fire pixels using a 15-km $\pm$30-min search radius, which is similar in concept to the "SCIT-filter" [16]. In addition, SCIT detections with a maximum reflectivity $>$ 45 dBZ are removed, and the reflectivity exceeding this value is very likely to be a result of precipitation or ground clutter. For the period of study selected here, this threshold was never exceeded. The "storm-top" parameter from the SCIT algorithm reports the highest level (in kilometers) for which 10 dBZ or greater reflectivity values were observed, which corresponds to an overall storm detection. The values are used to estimate the height to which ash and debris are being lofted. Unless otherwise noted, all height levels reported here have been converted to height ASL for consistency across all sensors.

It is very important to emphasize that we are not directly sampling smoke aerosols, but the larger biomass matter produced by the fire and lofted into the atmosphere by the fire [3]. Some of this BBD may have diameters of up to 1 cm, which accounts for much of the observed reflectivity. However, depending upon their size, the lifetime of such large biomass matter in the atmosphere is generally on the order of minutes before falling back to the ground [9]. Aerosols remain suspended in the atmosphere for longer periods of time when compared to the larger BBD. Smoke aerosols are much smaller and lighter than the particles associated with the radar reflectivity returns [9]. As a result, smoke aerosols are likely being transported higher into the atmosphere than indicated by the SCIT-derived heights or the radar cross section presented hereinafter.

MODIS level 1B reflectance (MOD02), level 2 aerosol data (MOD04) [17], and cloud top temperature (MOD06) [18] from the Terra and Aqua satellites are qualitatively compared with the radar data to determine the implications of large amounts of BBD being injected into the atmosphere on downstream aerosol and air-quality conditions. The HYbrid Single-Particle Lagrangian Integrated Trajectory (HYSPLIT) model is used to model the trajectory of parcels at several levels from one location backward or forward in time [19]. The atmospheric conditions are derived from archived rapid update cycle (RUC) model analyses, which have a spatial resolution of 20 km and are available every hour [20]. Finally, the radar results are compared with a single CALIPSO lidar overpass at 1914 UTC on May 24, 2007. CALIPSO does not overpass the fire-affected region at ideal times for the

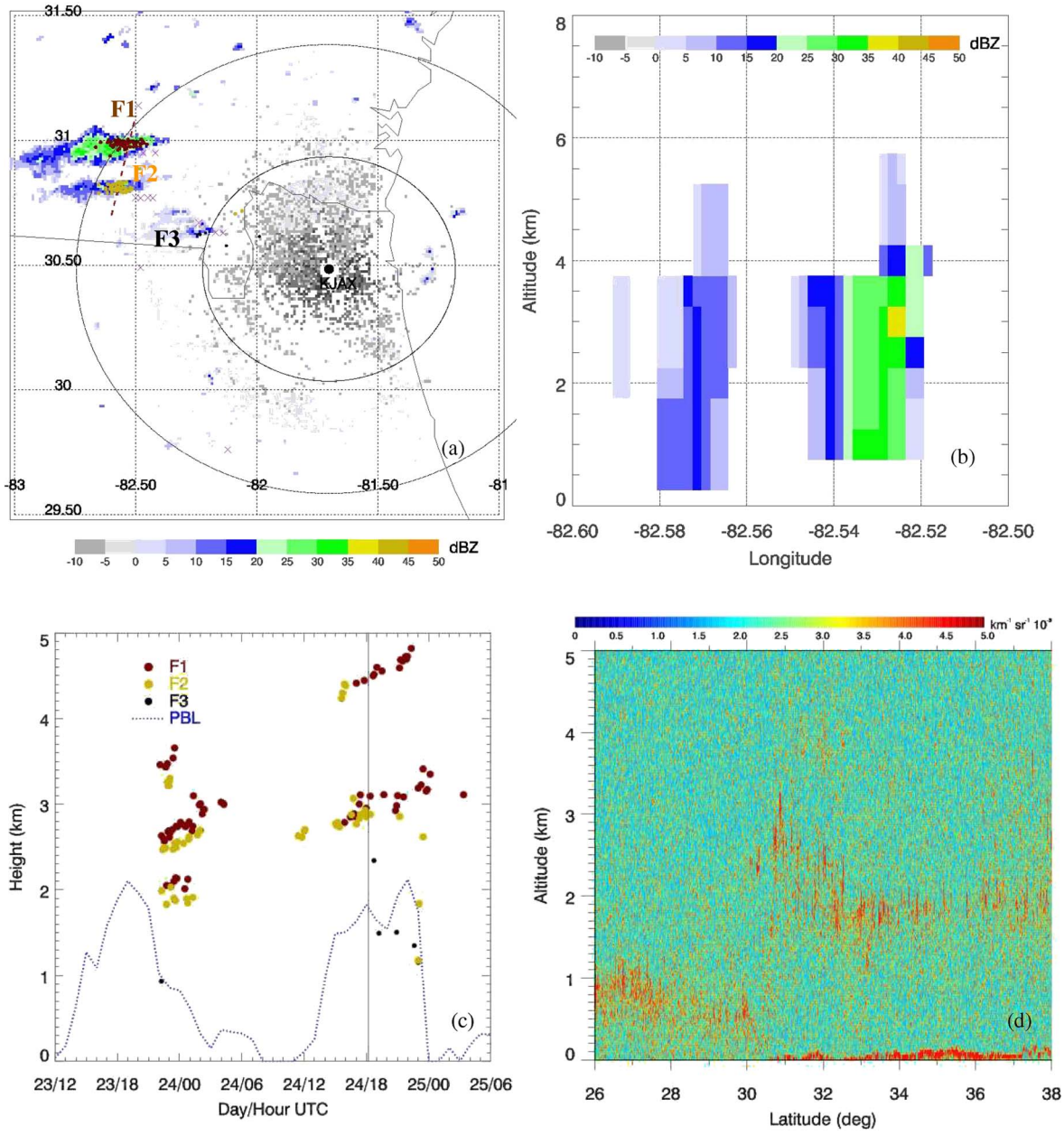

Fig. 3. (a) KJAX reflectivity at 1.5 km at 1812 UTC on May 24 showing two distinct BBD plumes in southern Georgia, ∼80 km northwest of the radar. Circles indicate 50- and 100-km range rings centered around the radar location. SCIT smoke detections are overlaid with dark red and yellow colors representing F1 and F2, respectively, with black dots indicating the smaller fire (F3). (b) Vertical cross section of reflectivity collected in VCP-21 corresponding to the dashed line in (a). Note that the northern fire has substantially greater reflectivity at all levels, with 5-dBZ returns extending to 5 km in altitude. (c) Time series versus height of SCIT BBD detections along with RUC planetary boundary layer heights between 2200 UTC on May 23 and 0600 UTC on May 25, with the vertical line denoting 1812 UTC. Injection heights for F1, F2, and F3 are plotted using the same color scheme used in panel (a). CALIPSO 532-nm backscatter reflectance as a function of latitude for 1914 UTC on May 24, 2007. (d) Aerosol layer is readily apparent around 2 km ASL from near the Gulf Coast (31° N) to northern Mississippi.

quantitative comparison of aerosol injection height versus BBD injection height, but is close enough to at least provide insight as to where the aerosols being injected into that atmosphere travel.

III. Results

The smoke plumes and surrounding cumulus clouds at roughly 1900 UTC on May 24, 2007 are visible from the Aqua MODIS level 1B data plotted in Fig. 2(a). The smoke plume is clearly evident in southeastern Georgia being transported westward by the prevailing winds and is visible more than 150 km downwind of the fire locations (denoted as red "X"s). The inset in Fig. 2(a) shows high-resolution (250-m) visible data with the MODIS cloud top temperatures overplotted. The boundary cumulus field is visible under the smoke plume near the fire (< 30 km), whereas a more complex smoke–cloud interaction seems to be occurring further downstream. At this time, the fires do not seem to be associated with significant pyro-cumulus, although some elevated cloud features associated with the smoke plume are present 50–60 km downstream of the fire. This is in contrast to the fires examined in [4], [5], and [6], where the overshooting pyro-cumulus tops are clearly evident near the fire.

The aerosol optical thicknesses (AOT) from Terra and Aqua, approximately 24 h afterward (16–1900 UTC on May 25), are plotted in Fig. 2(b) to emphasize the transport of the smoke from its source to long distances downstream. No aerosol retrievals could be made near the fire locations due to the presence of a large low-level cumulus cloud field and the difficulties in the MODIS retrieval algorithms for separating clouds from thick smoke plumes [21]. However, substantial aerosol concentrations (AOT $\sim$ 1.0) are retrieved in western Alabama and eastern Mississippi, downstream of the fire, as evident from the 800-hPa-level wind vectors. Note the relatively small spatial coverage of the fire and initial smoke plume compared to the much larger downwind coverage of high AOT. During this 32-h period, the GOES fire intensity information estimated that over 1 Tg of smoke was injected into the atmosphere. By 1800 UTC on May 25, the intensity of the fires significantly decreases, with only a few GOES fire pixels present and a very thin smoke layer to the southwest [Fig. 2(b)].

The reflectivity from the KJAX WSR-88D radar at 1812 UTC on May 24 (approximately 1:12 P.M. local time) at 1.5 km in altitude is shown in Fig. 3(a). Two distinct fire plumes are evident 80–100 km west–northwest of the radar (F1, F2). A third much weaker fire is present $\sim$50 km northwest of the radar (F3). The locations of these plumes correspond well with the GOES fire pixels (red "X"s) at this time, although the radar plumes are somewhat downwind of the fire pixels, as expected. The northernmost fire (F1) appears to be the strongest, with higher reflectivity values and greater aerosol coverage of detectable BBD. All of the BBD plumes are oriented in an east-to-west direction, which corresponds with the east-to-west wind flow present in the vicinity of the radar [Fig. 2(a)]. The analysis of the velocity characteristics of the plumes indicates that they were traveling away from the radar between 5 and 10 m s^{-1}, with the wind speed increasing with height. Using the RUC data, the tangential component of wind speed is estimated to be up to 5 m s^{-1}, which corresponds to a debris particle lifetime of approximately 1 h as debris are visible at least 50 km downwind of the strongest fire. However, given the lack of debris size and weight information, it is difficult to arrive at quantitative assessments of updraft velocity.

The northern fire is visible at the 2.4° elevation scan for a period of several hours, which corresponds to a height above 4 km at ranges beyond 80 km [Fig. 1(a) and (b)]. The southern fire generally exhibits weaker and lower reflectivity values. This can be visualized by examining a vertical cross section of radar data through the plumes of both fires at 1812 UTC on May 24 [Fig. 3(b)]. The northern fire is associated with greater reflectivity values at all levels and indicates $>$ 5 dBZ reflectivity to almost 6 km in altitude, which is well above the boundary layer height [Fig. 3(c)]. The large reflectivity values associated with the northern fire ($>$ 30 dBZ) indicate that very large concentrations of BBD and their associated aerosols are being lofted high into the atmosphere, which is in response to the localized instability produced by the heat of the fires.

The BBD injection heights between 2200 UTC on May 23 and 0600 UTC on May 25 are calculated using the SCIT output from every volume scan, which is filtered to remove precipitation and other nonsmoke-related detections. Several interesting trends are apparent in the time series of injection height [Fig. 3(c)]. First is that the detections are split up into two separate temporal groupings, one between 2200 UTC on May 23 and 0400 UTC on May 24, and the second between 1500 UTC on May 24 and 0100 UTC on May 25. These groups locally correspond to the late afternoon and early evening time period, i.e., when convective turbulence and boundary layer height are maximized, as indicated by the hourly RUC-derived planetary boundary layer height [Fig. 3(c)] averaged over the region bounded by the inset in Fig. 2(a). During the first period, the detected BBD injection heights are clustered around 2.5–3 km, with a few significant differences ($>$ 1 km) in height between the two primary fires. The small differences are primarily a function of range from the radar and are more evident when the radar is in VCP-21 (after 0900 UTC), which has a lower vertical resolution. If the lofted BBD is detected at the 1.45° elevation at 80 and 100 km, then the latter will have a higher BBD height value, assuming no reflectivity returns at higher elevation scans. This does increase the uncertainty associated with this technique, particularly when data from only a single radar are used.

During the nighttime hours, the intensity of the fires decreases, and the lower atmosphere becomes increasingly stable due to the cooling surface temperatures. An analysis of the radar data and corresponding GOES fire counts during this time also shows very little evidence for the fires at night, which indicates that the amount of ash (and likely aerosols too) being lofted into the atmosphere is much less than during the daytime hours. As a result, SCIT no longer reports BBD injection heights during this period. After 1500 UTC on May 24, the intensity of the fires begins to increase again. The initial injection height detections are approximately 3 km ASL, similar to the previous time period. However, detections reaching up to 4.5 km are soon evident, inserting BBD and aerosols well above the ambient boundary layer height, which is approximately 2 km [Figs. 2(a) and 3(c)]. Initially, these are from the southern fire (F2), but soon after, the detections at this altitude solely result from the northern fire (F1) [Fig. 3(a) and (c)]. Note that the injection heights at both $\sim$3- and 4.5-km levels are recorded with the northern fire. This difference is a function of the SCIT algorithm finding a 10-dBZ reflectivity associated with a smoke plume from either the 1.45° or 2.4° elevation data. At the time of the radar cross section (1812 UTC), the injection height for the northern fire was 4.5 km, which is consistent with the 10-dBZ contour in Fig. 3(b). The variability in injection height for a single plume is not unexpected and reflects the extreme temporal variability of BBD concentrations near the fire source. The maximum injection height for the northern fire remains $\sim$4.5 km until approximately 0000 UTC on May 25. Both fires rapidly decrease in intensity thereafter, with only a single detection after 0100 UTC. By 1800 UTC on May 25, the GOES data indicate that the number of fires has substantially decreased, with only a residual smoke evident from the MODIS data [Fig. 2(b)].

"Cloud top temperatures" at 1900 UTC derived from the MODIS (MYD06) cloud product are overlaid on the high-resolution inset in Fig. 2(a). The thickness of the smoke plume and its possible interaction with cumulus clouds leads the MODIS algorithm to classify the plume as "clouds" rather than "aerosols." Cloud top temperatures below -15 °C are located within the smoke plume, which corresponds to an attitude of

5–6 km. What remains of the smoke plume by May 25 is much warmer (0 °C) and nearer to the surface, since the injection of new aerosols several kilometers into the atmosphere is no longer occurring [Fig. 2(b)]. Recall that the algorithm-derived injection height from the northern fire was approximately 4.5 km around 1900 UTC on May 24; thus, the method employed here seems to underestimate the maximum smoke aerosol injection height by approximately 1 km. Increasing the sensitivity of the algorithm by lowering the reflectivity threshold would result in higher algorithm-derived injection heights, since a 0- to 10-dBZ reflectivity is present with the debris plume at an altitude of 5.5 km. A limited number of plume detections are present the weaker fire closer to the radar, with heights only reaching ∼1 km. Both radar data and GOES fire data indicate that this fire is much weaker. Thus, it is less likely to transport significant aerosol concentrations into the free atmosphere (i.e., above the boundary layer). While these statistics only represent a single case study, they do indeed suggest that the radar is a very useful tool for providing injection heights for smoke, although it is not directly sensitive to the smoke aerosols themselves.

Unfortunately, no CALIPSO or MISR overpass occurred directly over the sources of the fire to allow a full quantitative assessment of radar-derived injection heights during the period of study. However, a CALIPSO overpass did occur in western Alabama at 1914 UTC on May 24, showing a combined cloud and aerosol layer near 2 km ASL north of 31° N [Fig. 3(d)]. The boundary layer heights along the CALIPSO track range anywhere from 0 to 2 km, but the zero values around 32° N are a result of no heights being derived by RUC. Where positive values do exist, RUC indicates the boundary layer to be mostly between 1.5 and 2 km above the surface [Fig. 2(a)]. Significant cloud cover exists along the CALIPSO track, but patches of high AOT (> 0.5) are also evident in between the clouds. The level 2 CALIPSO product also indicates that a mix of clouds and aerosols exists within this layer. To determine the source of these aerosols along the CALIPSO overpass, the HYSPLIT model along with meteorological data archives from the Air Resources Laboratory was used to calculate the trajectory of an atmospheric parcel from a point in western Alabama ($32.5°$ N, $-88.0°$ W) at 1900 UTC on May 24 at 2 km in altitude backward in time 24 h. The modeled trajectory traces back to a point near the Georgia fires at approximately 0300 UTC on May 24, 16 h prior to the CALIPSO overpass [Fig. 2(a)]. The parcel height increases as one travels from the initialization location to regions nearer the fires, indicating that a lower-level air quality is being impacted by aerosols originating from a higher level. Recall that the radar-derived BBD injection height prior to 0300 UTC on May 24 was between 3 and 4 km [Fig. 3(c)]. This agrees well with the HYSPLIT analysis that shows a parcel being injected near 3 km in height at 0300 UTC on May 24 near the fire descending to ∼2 km, where CALIPSO observes the aerosol and cloud layer in western Alabama at 1900 UTC.

While no MISR overpasses of the fire occurred during the period of study, it was possible to compare our methods with the September 4, 2003 case analyzed in detail in [4]. During this day, several wildfires were observed in central Oregon, producing smoke plumes extending > 100 km downwind of the individual fires. At the time of the MISR overpass (∼1930 UTC), the stereo height product reported an aerosol layer (mixed with pyro-cumulus) around 5 km above the surface near the source of the fire. This fire also happened to be observable from the KTRX WSR-88D radar 150 km to the northwest. At this range, the WSR-88D poorly samples the lowest 2 km of the atmosphere, which means that significant BBD concentrations likely exist above this level. The WSR-88D observations at this time show reflectivity returns of > 0 dBZ at least 4 km above the ground level at the same location as the 5-km MISR estimate. Given that the radar is observing much larger and heavier particles than the MISR, this level of agreement is encouraging, and as expected, the radar-derived height is somewhat below the MISR value. Interestingly, even higher BBD injection heights (∼7 km above the ground level) are observed closer to 2330 UTC on September 4, further emphasizing the importance of high temporal resolution in wildfire observations not available with satellite observations.

IV. Conclusion

Using WSR-88D radar data, we have shown that it is possible to estimate the injection height of BBD (a possible surrogate for smoke aerosols) in the atmosphere from biomass burning. A modified version of the SCIT algorithm was able to objectively calculate the BBD injection heights for several fires in southern Georgia between May 23 and 25, 2007. A strong diurnal variability in fire intensity exists, with the strongest reflectivity observed during the late afternoon and evening hours. The SCIT-derived BBD injection heights ranged between 3 and 5 km ASL for the two most significant fires. The strongest (northern) fire generated measurable reflectivity above 5 km for several hours between 1700 UTC on May 24 and 0000 UTC on May 25. An analysis of MODIS aerosol optical thickness indicates that the smoke from these fires is transported into western Alabama and eastern Mississippi between 1200 UTC on May 24 and 1200 UTC on May 25. According to HYSPLIT-modeled parcel trajectories, at least a portion of the aerosol layer observed by CALIPSO originates from the fire region located more than 500 km away, ∼18 h previously, from a height of ∼3 km. This is in excellent agreement with the SCIT-derived plume heights reported at this time. A similar agreement was observed with MISR stereo height observations of the September 4, 2003 wildfire in Oregon, where BBD was evident upward of 5 km above the ground level.

Several sources of uncertainty remain before radars can be used to determine BBD and aerosol injection height from radar data with a high degree of certainty. As the range increases, the uncertainty in height measurements also increases, whereas the sensitivity to low-level phenomena decreases. Future research will utilize data from multiple radars to at least partially overcome this problem and to also retrieve the 3-D wind field associated with each smoke plume. The question also remains as to whether the 10-dBZ threshold is a good indicator of BBD injection height. Currently, combined BBD particle distributions and S-band radar reflectivity data sets do not exist to quantitatively make this comparison, but time will eventually provide the necessary data.

The greatest uncertainty lies in the exact relationship between the vertical distribution of larger ash particles and smaller

lighter smoke aerosols. The ash and debris from the fire only remain suspended in the atmosphere for an hour or less, whereas the smoke may remain for days. However, the intensity of the fire, the amount of ash it produces, and the amount of smoke it injects into the atmosphere are all directly related. MODIS cloud top temperatures below $-15\ ^{\circ}\mathrm{C}$ are observed within the smoke plume, which is further evidence supporting the radar observations of injection heights in excess of 5 km.

It is left to future research to fully address the details of this relationship, as it will require much larger data sets across a greater variety of sensors than the research presented here. Overall, this paper provides a framework for the use of widely available radar data, as an independent source, to estimate the height of ashlike particles ($D \sim 1$ km) that are being injected into the atmosphere from biomass burning. Continuing research will attempt to estimate smoke aerosol injection heights and vertical distributions from the radar observations of larger particles, which would be very useful for satellite studies of particulate-matter air quality and numerical modeling simulations that require such information.

ACKNOWLEDGMENT

The authors would like to thank V. "Starry" Manoharan for preprocessing the MODIS level 1B data displayed in Fig. 2, and the helpful comments provided by the anonymous reviewers. The MODIS data were obtained from the Level 1 and Atmosphere Archive and Distribution System (LAADS) at the NASA Goddard Space Flight Center.

REFERENCES

[1] J. Wang, S. A. Christopher, U. S. Nair, J. S. Reid, E. M. Prins, J. Szykman, and J. L. Hand, "Mesoscale modeling of Central American smoke transport to the United States: 1. 'Top-down' assessment of emission strength and diurnal variation impacts," *J. Geophys. Res.*, vol. 111, no. D5, p. D05 S17, Mar. 2006. DOI: 10.1029/2005JD006416.

[2] M. Vaughan, S. Young, D. Winker, K. Powell, A. Omar, Z. Liu, Y. Hu, and C. Hosteler, "Fully automated analysis of space-based lidar data: An overview of CALIPSO retrieval algorithms and data products," *Proc. SPIE*, vol. 5575, pp. 16–30, Nov. 2004.

[3] R. M. Banta, L. D. Olivier, E. T. Holloway, R. A. Kropfli, B. W. Bartram, R. E. Cupp, and M. J. Post, "Smoke-column observations from two forest fires using Doppler lidar and Doppler radar," *J. Appl. Meteorol.*, vol. 31, no. 11, pp. 1328–1349, Nov. 1992.

[4] R. A. Kahn, W. H. Li, C. Moroney, D. J. Diner, J. V. Martonchik, and E. Fishbein, "Aerosol source plume physical characteristics from space-based multiangle imaging," *J. Geophys. Res.*, vol. 112, no. D11, p. D05 S17, Jun. 2007. DOI: 10.1029/2006JD007647.

[5] M. Fromm, R. Bevilacqua, R. Servranckx, J. Rosen, J. P. Thayer, J. Herman, and D. Larko, "Pyro-cumulonimbus injection of smoke to the stratosphere: Observations and impact of a super blowup in northwestern Canada on 3–4 August 1998," *J. Geophys. Res.*, vol. 110, no. D8, p. D08 205, Apr. 2005. DOI: 10.1029/2004JD005350.

[6] M. Fromm, A. Tupper, D. Rosenfeld, R. Servranckx, and R. McRae, "Violent pyro-convective storm devastates Australia's capital and pollutes the stratosphere," *Geophys. Res. Lett.*, vol. 33, no. 5, p. L05 815, Mar. 2006. DOI: 10.1029/2005GL025161.

[7] J. E. Penner, R. J. Charlson, J. M. Hales, N. S. Laulainen, R. Liefer, T. Novakov, J. Ogren, L. F. Radke, S. E. Schwartz, and L. Travis, "Quantifying and minimizing uncertainty of climate forcing by anthropogenic aerosols," *Bull. Amer. Meteorol. Soc.*, vol. 75, no. 3, pp. 375–400, Mar. 1994.

[8] D. Mazzoni, J. Logan, D. Diner, R. A. Kahn, L. Tong, and Q. Li, "A data-mining approach to cataloging smoke plumes from MISR and MODIS data," *Remote Sens. Environ.*, vol. 107, no. 1/2, pp. 138–158, Mar. 2007.

[9] G. G. L. Hufford, H. L. Kelley, W. Sparkman, and R. K. Moore, "Use of real-time multisatellite and radar data to support forest fire management," *Weather Forecast.*, vol. 13, no. 3, pp. 592–605, Sep. 1998.

[10] T. A. Jones, S. A. Christoper, and W. Petersen, "Dual polarimetric and dual wavelength radar characteristics of an apartment fire," *J. Atmos. Ocean. Technol.*, 2009. to be published.

[11] V. M. Melnikov, D. S. Zurnic, and R. M. Rabin, "Radar polarimetric signatures of wildfire plumes," *Geophys. Res. Lett.*, vol. 35, no. 14, p. L14 815, Jul. 2008. DOI:10.1029/2008GL034311.

[12] T. D. Crum and R. L. Alberty, "The WSR-88D and the WSR-88D operational support facility," *Bull. Amer. Meteorol. Soc.*, vol. 74, no. 9, pp. 1669–1687, Sep. 1993.

[13] R. J. Doviak and D. S. Zrnic, *Doppler Radar and Weather Observations: Second Edition*. San Diego, CA: Academic, 1993.

[14] E. M. Prins and W. P. Menzel, "Trends in South American biomass burning detected with the GOES Visible Infrared Spin Scan radiometer atmospheric sounder from 1983 to 1991," *J. Geophys Res.*, vol. 99, no. D8, pp. 16 719–16 735, 1994.

[15] J. T. Johnson, P. L. MacKeen, A. Witt, D. Mitchell, G. J. Stumpf, M. D. Eilts, and K. W. Thomas, "The storm cell identification and tracking algorithm: An enhanced WSR-88D algorithm," *Weather Forecast.*, vol. 13, no. 2, pp. 263–276, Jun. 1998.

[16] T. A. Jones, K. M. McGrath, and J. T. Snow, "Association between NSSL mesocyclone detection algorithm-detected vortices and tornadoes," *Weather Forecast.*, vol. 19, no. 5, pp. 872–890, Oct. 2004.

[17] R. C. Levy, L. A. Remer, S. Mattoo, E. F. Vermote, and Y. J. Kaufman, "Second-generation operational algorithm: Retrieval of aerosol properties over land from inversion of Moderate Resolution Imaging Spectroradiometer spectral reflectance," *J. Geophys. Res.*, vol. 112, no. D13, p. D13 211, Jul. 2007. DOI: 10.1029/2006JD007811.

[18] S. Platnick, M. D. King, S. A. Ackerman, W. P. Menzel, B. A. Baum, J. C. Riedi, and R. A. Frey, "The MODIS cloud products: Algorithms and examples from Terra," *IEEE Trans. Geosci. Remote Sens.*, vol. 41, no. 2, pp. 459–473, Feb. 2003.

[19] R. R. Draxler, "Evaluation of an ensemble dispersion calculation," *J. Appl. Meteorol.*, vol. 42, no. 2, pp. 308–317, Feb. 2003.

[20] S. G. Benjamin, D. Devenyi, S. S. Weygandt, K. J. Brundage, J. M. Brown, G. A. Grell, D. Kim, B. E. Schwartz, T. G. Smirnova, T. L. Smith, and G. S. Manikin, "An hourly assimilation–forecast cycle: The RUC," *Mon. Weather Rev.*, vol. 132, no. 2, pp. 495–518, Feb. 2004.

[21] J. I. Brennan, Y. J. Kaufman, I. Koren, and R. R. Li, "Aerosol-cloud interaction—Misclassification of MODIS clouds in heavy aerosol," *IEEE Trans. Geosci. Remote Sens.*, vol. 43, no. 4, pp. 911–915, Apr. 2006.

Thomas A. Jones received the B.S. and M.S. degrees in meteorology (while focusing on the development of regional thunderstorm climatologies) from the University of Oklahoma, Norman, in 2000 and 2002, respectively, and the Ph.D. degree in atmospheric science (while specializing in improving hurricane intensity change forecasts using satellite-derived passive microwave imagery) from The University of Alabama in Huntsville (UAH), Huntsville, in May 2006.

Since May 2006, he has been a Research Scientist with the Department of Atmospheric Sciences, UAH. He has a wide range of research interests within the atmospheric science community. He is currently doing research on the effects of aerosols and their subspecies on shortwave and longwave radiative effects using MODIS and CERES data. This research is currently being expanded to include the effects of aerosols on clouds.

Sundar A. Christopher received the Ph.D. degree in atmospheric science from Colorado State University, Fort Collins.

He is currently a Professor with the Department of Atmospheric Sciences and the Associate Director of the Earth System Science Center, The University of Alabama in Huntsville (UAH), Huntsville. His research interests include satellite remote sensing of clouds and aerosols and their impact on air quality and global and regional climates.